Phase-shift calculation of ionized impurity scattering in semiconductors

J. R. Meyer and F. J. Bartoli
Naval Research Laboratory, Washington, D.C. 20375
(Received 10 November 1980)

Partial-wave phase shifts for the scattering of electrons and holes of arbitrary degeneracy by a screened Coulomb potential have been calculated assuming isotropic, parabolic energy bands. For free particles in the effective-mass approximation, all such interactions can be characterized by two parameters. At each point in this two-dimensional space, two final results have been obtained from which the transport integrals can be evaluated. One is a sum of the phase shifts which must be employed in satisfying the Friedel sum rule, while the other corresponds to the total momentum-transfer cross section due to all partial waves. For a parametric space which includes nearly all experimental conditions of interest, these results are presented in approximate analytic form. Over a broad range of electron and hole concentrations and temperatures in Ge, Si, and GaAs, comparison is made between ionized-impurity mobilities calculated from the phase shifts and those obtained in the Born approximation.

I. INTRODUCTION

Brooks-Herring theory[1,2] has been used extensively in calculating ionized-impurity mobilities in semiconductors. While one obtains simple analytic expressions for the scattering cross section, the Born approximation employed in this theory is invalid for many experimental conditions of interest. An attractive alternative is the partial-wave phase-shift method, which yields an essentially exact solution to the scattering problem for a specific potential. This technique was first applied to the screened Coulomb potential by Blatt,[3] who calculated phase-shift cross sections for various values of the scattering parameters. While Blatt's results apply mostly to nondegenerate semiconductors, Csavinszky[4] employed a variational technique to obtain analytic approximations for the zero-order phase shifts in the limit of extreme degeneracy. Neither of these authors attempted to satisfy the Friedel sum rule.[5] This shortcoming was corrected by Krieger and Strauss,[6] who provided an essentially "complete" phase-shift treatment for the scattering of degenerate electrons by a screened Coulomb potential. Because scattering in the extreme degenerate limit can be formulated in terms of only one parameter,[7] Krieger and Strauss were able to present a universal curve for the ratio between the resistivity obtained from the phase-shift method compared to the Born approximation result. In the case of arbitrary degeneracy a comprehensive treatment is more difficult since two independent parameters are required.[3] Boardman and Henry[8] have performed the phase-shift analysis for the nondegenerate scattering problem, using the generalized Friedel sum rule.[9] However, they reported only sample calculations rather than general results. Thus, while a number of phase-shift treatments of ionized-impurity scattering have been reported, it is not possible to employ previously published work to obtain quantitative transport results in any extended regime except that of extreme degeneracy.

Presented in the following sections is a comprehensive treatment of electron scattering by the screened Coulomb potential. For broad ranges of the two independent parameters, total scattering cross sections are calculated from the partial-wave phase shifts. Weighted sums of the phase shifts are also presented so that the generalized Friedel sum rule can be satisfied for electrons or holes of arbitrary degeneracy. Results are given in approximate analytic form in order to minimize the tabular material which must be presented. Using the final expressions, scattering probabilities can be calculated for almost any experimental conditions of interest. As an illustration, the cross sections obtained are applied to ionized-impurity scattering of electrons and holes in Ge, Si, and GaAs for a broad range of temperatures and doping levels. The resulting mobilities are given primarily for comparison with the Born approximation, since mechanisms other than ionized-impurity scattering are ignored. However, for the cases of n-type silicon, GaAs, and ZnSe, detailed comparisons between a complete transport theory and experiments will be provided in later publications.[10]

II. THE PARTIAL-WAVE FORMALISM

The Schrödinger equation for a free electron or hole of scalar effective mass m^* in the presence of a scattering potential $V(r)$ can be written

$$\left(\frac{-\hbar^2}{2m^*}\nabla^2 + V(r)\right)u = Eu\,, \tag{2.1}$$

where E is the particle's total energy. For a radially symmetric potential, the wave function u may be expanded

$$u(\vec{r}) = \sum_{lm} B_{lm} S_l(r) Y_{lm}(\theta, \phi) \tag{2.2}$$

where the Y_{lm} are spherical harmonics. The radial part of Eq. (2.1) can then be separated from the angular part, giving

$$\left(\frac{-\hbar^2}{2m^*r^2}\frac{\partial}{\partial r} r^2 \frac{\partial}{\partial r} + \frac{l(l+1)\hbar^2}{2m^*r^2} + V(r)\right) S_l = \frac{\hbar^2 k^2}{2m^*} S_l , \tag{2.3}$$

where the quantity k^2 is introduced through the definition $E = \hbar^2 k^2/2m^*$. If the new variables $x \equiv kr$ and $R_l \equiv xS_l$ are introduced, Eq. (2.3) becomes

$$\frac{-\partial^2 R_l}{\partial x^2} + \left(\frac{l(l+1)}{x^2} + U(x) - 1\right) R_l = 0 , \tag{2.4}$$

where $U(x) \equiv V(r)/E$. This form has the advantage that the normalized potential $U(x)$ contains all dependence on the material properties of the semiconductor.

It can be shown that for a vanishing potential the general solution to Eq. (2.4) is[11]

$$R_l \to x[A_l j_l(x) + B_l n_l(x)], \tag{2.5}$$

where j_l and n_l are spherical Bessel functions. Here $B_l = 0$ in order to satisfy the boundary condition that R_l/x be well behaved at the origin. At large x, Eq. (2.5) has the asymptotic form $R_l \to \sin(x - \frac{1}{2} l\pi)$. If one now introduces a potential $U(x)$ with finite range, the solution at large x must still have the form of Eq. (2.5), except that $B_l \neq 0$. It can be shown that in the large x limit R_l becomes

$$R_l \to \sin(x - \tfrac{1}{2} l\pi + \delta_l), \tag{2.6}$$

where δ_l is known as the phase shift of the lth partial wave. The δ_l must be determined from a solution of the radial wave equation (2.4).

It is well known that the scattering amplitude $f(\theta)$ depends on the phase shifts through the relation[11]

$$f(\theta) = \frac{1}{2ik} \sum_{l=0}^{\infty} (2l+1)(e^{2i\delta_l} - 1) P_l(\cos\theta), \tag{2.7}$$

where θ is the angle between the incoming and outgoing particles and P_l is the Legendre polynomial of order l. The differential scattering cross section

$$\sigma(\theta) = |f(\theta)|^2 \tag{2.8}$$

can then be employed to determine the total momentum-transfer cross section

$$\sigma_T = 2\pi \int_0^{\pi} \sigma(\theta)(1 - \cos\theta) \sin\theta \, d\theta . \tag{2.9}$$

It was first shown by Huang[12] that the integral of Eq. (2.9) can be performed analytically to yield the relatively simple result

$$\sigma_T = \frac{4\pi}{k^2} \sum_{l=0}^{\infty} (l+1) \sin^2(\delta_l - \delta_{l+1}) . \tag{2.10}$$

That is, once the phase shifts have been determined from Eq. (2.4), the scattering cross section is easily evaluated.

So far, this discussion has been general with respect to the choice of a potential. We now consider the specific case of a screened Coulomb interaction

$$V(r) \equiv q_i Z_I \frac{e^2}{\kappa_0 r} e^{-r/\lambda_s} , \tag{2.11}$$

where q_i and Z_I are the charges of the mobile carrier and ionized impurity in units of e, and κ_0 is the static dielectric constant. For the screening length λ_s we write $\lambda_s = \lambda_0/\lambda_q$, where λ_q is an adjustable screening parameter (discussed below) and λ_0 is the Born approximation screening length[13]

$$\lambda_0^{-2} = \frac{4\pi e^2}{\kappa_0 k_B T} \left(n \frac{\mathcal{F}_{-1/2}(\eta_n)}{\mathcal{F}_{1/2}(\eta_n)} + p \frac{\mathcal{F}_{-1/2}(\eta_p)}{\mathcal{F}_{1/2}(\eta_p)} \right), \tag{2.12}$$

where n and p are the electron and hole densities, $\eta_i \equiv E_{Fi}/k_B T$ is the reduced Fermi energy, and $\mathcal{F}_r$ is the Fermi integral of order r.[14] With Eq. (2.11), the normalized potential $U(x)$ can be written

$$U(x) \equiv \frac{V(r)}{E} = -\frac{1}{xy} e^{-2x/b^{1/2}} , \tag{2.13}$$

where we have introduced the definitions

$$y \equiv -\tfrac{1}{2} k a_0 \frac{|Z_I|}{q_i Z_I} \tag{2.14}$$

$$b \equiv 4k^2 \lambda_s^2 , \tag{2.15}$$

where a_0 is the effective *Bohr* radius

$$a_0 = \frac{\hbar^2 \kappa_0}{m^* |Z_I| e^2} . \tag{2.16}$$

For an attractive potential $y = \frac{1}{2} k a_0$, whereas for a repulsive potential $y = -\frac{1}{2} k a_0$. It is useful to introduce the additional parameter

$$F \equiv \frac{b^{1/2}}{2|y|} = \frac{2\lambda_s}{a_0} = \frac{2\lambda_0}{\lambda_q a_0} . \tag{2.17}$$

In the discussion which follows, the differential equation (2.4) will be treated in terms of the three independent parameters l, y, and $F(\lambda_q)$. The value of the adjustable screening parameter λ_q must be determined from the generalized Friedel sum rule, which was first obtained by Stern.[9]

The sum rule can be understood in terms of the following picture[8,15] involving a plasma of free electrons in the presence of a donor ion. Each electron state is characterized by four quantum numbers n, l, m, and s. The l and m are indices

of the spherical harmonic $Y_{lm}(\theta, \phi)$ which appears in the electron wave function [see Eq. (2.2)], s is the spin state (not explicitly included above), while n characterizes the various solutions to the radial wave equation $R_l(k_{nl}r)$. Although wave vector k_{nl} has been treated in the discussion above as if it were continuous, it is in fact quantized. Employing the boundary condition that $R_l \to 0$ at the surface of a large sphere with radius $r = R$, one finds that in the absence of a potential the k_{nl}^0 must satisfy $k_{nl}^0 R = X_{nl}$, where X_{nl} is the nth zero of $j_l(x)$. In the presence of the potential $U(x)$, each zero at large x is displaced by the phase shift δ_l: $k_{nl}R = X_{nl} - \delta_l$.

To derive the generalized sum rule for arbitrary degeneracy, we note that the total electron density in the absence of the potential is given by

$$N_0 = 2\nu_e \sum_{l=0}^{\infty} \sum_{n=0}^{\infty} (2l+1) f_0(z_{nl}^0) , \tag{2.18}$$

where the sums over m and s have already been performed. Here ν_e is the number of degenerate electron valleys, $f_0(z) = (1 + e^{z-\eta})^{-1}$ is the Fermi distribution function, and z_{nl}^0 is the reduced energy for an eigenstate characterized by the quantum numbers n and l:

$$z_{nl}^0 = \frac{E_{nl}}{k_B T} = \frac{\hbar^2 X_{nl}^2}{2m^* k_B T R^2} . \tag{2.19}$$

If we now introduce the potential, z_{nl}^0 in Eq. (2.19) must be replaced by z_{nl}:

$$\begin{aligned} z^{nl} &= \frac{\hbar^2}{2m^* k_B T R^2} (X_{nl} - \delta_l)^2 \\ &\approx \frac{\hbar^2}{2m^* k_B T R^2} (X_{nl}^2 - 2X_{nl}\delta_l) . \end{aligned} \tag{2.20}$$

The Friedel sum rule states that the additional electron charge which is present within the sphere of radius R due to the perturbing effects of the potential, must be equal and opposite to the donor charge Z_I. That is, the donor must be completely screened at large r. We thus have

$$\begin{aligned} Z_I &= -q_e(N - N_0) \\ &= -2\nu_e q_e \sum_{l=0}^{\infty} \sum_{n=0}^{\infty} (2l+1)[f_0(z_{nl}) - f_0(z_{nl}^0)] \\ &\to -2\nu_e q_e \sum_{l=0}^{\infty} \sum_{n=0}^{\infty} (2l+1) \frac{\hbar^2 X_{nl} \delta_l}{m^* k_B T R^2} \left(\frac{-\partial}{\partial z_{nl}} f_0(z_{nl}) \right) . \end{aligned} \tag{2.21}$$

Using the property[16]

$$X_{nl} = k_{nl}R + \delta_l \xrightarrow[R \to \infty]{} (n + \tfrac{1}{2} l)\pi \approx n\pi ,$$

the sum over n can be converted to an integral over the reduced energy $z \equiv E/k_B T = \hbar^2 n^2 \pi^2 / (2m^* k_B T R^2)$. One finally obtains for the generalized Friedel sum rule

$$Z_I = -\frac{2\nu_e q_e}{\pi} \int_0^{\infty} dz\, f_0(1 - f_0) S(z, \lambda_q) , \tag{2.22}$$

where

$$S(z, \lambda_q) \equiv \sum_{l=0}^{\infty} (2l+1) \delta_l [y(z), F(\lambda_q)] . \tag{2.23}$$

The sum rule is satisfied by varying the adjustable screening parameter λ_q in calculating δ_l until both sides of Eq. (2.22) are equal. The same δ_l (y, F) are then used in Eq. (2.10) to obtain the total scattering cross section σ_T. For degenerate electrons with $\nu_e = 1$, Eq. (2.22) reduces to the result originally obtained by Friedel[5]:

$$Z_I = \frac{2}{\pi} \sum_{l=0}^{\infty} (2l+1) \delta_l (y_F, F) , \tag{2.24}$$

where $y_F = \frac{1}{2} k_F a_0$ and k_F is the Fermi wave vector.

Our solution to the scattering problem can thus be expressed in terms of two results: the total scattering cross section σ_T which is given by Eq. (2.10), and the quantity $S(z, \lambda_q)$ which is defined in Eq. (2.23) and is needed to satisfy the Friedel sum rule. Note that for a particular set of experimental conditions, we need not know each individual phase shift but only the two weighted sums which appear in the expressions for σ_T and S. It is convenient to normalize these sums to the corresponding Born approximation results. For example, the total Born cross section is[6]

$$\sigma_T^B(y, F) = \frac{\pi}{2k^2 y^2} \left(\ln(b+1) - \frac{b}{b+1} \right) . \tag{2.25}$$

We therefore define the normalized cross section

$$\begin{aligned} H_0(y, F) &\equiv \sigma_T / \sigma_T^B \\ &= \frac{8y^2 \sum_{l=0}^{\infty} (l+1) \sin^2[\delta_l(y, F) - \delta_{l+1}(y, F)]}{\ln(b+1) - b/(b+1)} \end{aligned} \tag{2.26}$$

Similarly, the phase shifts which one obtains in the Born approximation[17]

$$\delta_{lB}(y, F) = \frac{1}{y} \int_0^{\infty} j_l^2(x) x e^{-2x/b^{1/2}} , \tag{2.27}$$

can be used in Eq. (2.23) to give the Born result[18] $S^B = F^2 y$. By analogy to Eq. (2.26), we define the normalized sum

$$S_0(y, F) \equiv \frac{S}{S^B} = \frac{1}{F^2 y} \sum_{l=0}^{\infty} (2l+1) \delta_l (y, F) . \tag{2.28}$$

Hence the generalized Friedel sum rule can be written

$$Z_I = -\frac{2}{\pi}\sum_i \nu_i q_i F_i^2(\lambda_q)\int_0^\infty dz\, f_0(1-f_0)y_i(z),\quad y_i, F_i), \tag{2.29}$$

where the index i has been included to account for the possibility of simultaneous screening by more that one species of carrier, such as some combination of electrons, heavy holes, and light holes.

As discussed in the following section, $S_0(y,F)$ and $H_0(y,F)$ have been evaluated for a very broad range of y and F. The foregoing analysis has demonstrated that these two results represent a complete solution to the problem of free-particle scattering by a screened Coulomb potential.

III. EVALUATION OF THE PHASE SHIFTS

Boardman and Henry[8] have pointed out that when Eq. (2.4) is solved numerically, one must often integrate to very large r before the wave function obtains the form of a sine function as in Eq. (2.6). We have therefore employed a technique discussed by those authors which allows one to find the phase shifts as soon as the integration has proceeded beyond the range of the potential.

With respect to convergence in l, several previous authors have asserted that $\delta_l - \delta_{lB}$ converges rapidly with increasing l, so that only a few low-order phase shifts must be calculated. While we found this to be true under certain conditions, notably for extreme degeneracy, convergence is quite slow in other experimentally interesting regions of the yF space. For this reason, up to 49 phase shifts were calculated numerically by computer. In cases for which additional phase shifts were required, the error proved to be acceptable when the Born values δ_{lB} were employed for $l \geq 50$.

As shown in the previous section, the solution for scattering by a screened Coulomb potential can be considered generally in terms of $S_0(y,F)$ and $H_0(y,F)$, which are defined in Eqs. (2.28) and (2.26), respectively. We have evaluated $S_0(y,F)$ and $H_0(y,F)$ to within 1% computational error for $|y| \geq 0.01$ and $0.1 < F < 400$, a range sufficiently broad to cover virtually all conditions of experimental interest. The derived quantities are plotted in Figs. 1–6 as functions of y for various constant values of F.

Figures 1–6 can be used to estimate the correction of the phase-shift cross section to the Born approximation result. However, it is impractical to use the graphical data in detailed calculations of electron and hole mobilities. For this reason, approximate analytic models have been obtained by fitting to the calculated results for S_0 and H_0. These are presented in the Appendix. In the well behaved regions of Figs. 1–6, the error introduced by the modeling is at most a few percent. However, at small y and large F the functions show wild oscillations in both parameters. In this region, the presentation of highly accurate modeling would require a prohibitive amount of tabular material. At present, such an effort does not seem worthwhile since the regime is difficult to reach experimentally. Although the models in this region show the same oscillating structure as the exact functional forms of S_0 and H_0 (as represented by the figures), the precise magnitude of the model cross sections should not be taken too seriously at $0.01 \leq y \leq 0.1$ and $F \geq 3.5$. For all regions, the maximum modeling errors are specified in the Appendix. Special care was taken to assure that the error is held to a minimum in the crossover region where the Born approximation is just beginning to become invalid.

In order to understand the behavior of the functions $S_0(y,F)$ and $H_0(y,F)$ which are illustrated in Figs. 1–6, we now make some qualitative observations concerning the solution to the differential equation (2.4) for the lth partial wave. It can be shown that Eq. (2.4) is equivalent to the integral equation[17]:

$$\sin\delta_l = \frac{1}{y}\int_0^\infty R_l(x) j_l(x) e^{-2x/b^{1/2}}\, dx. \tag{3.1}$$

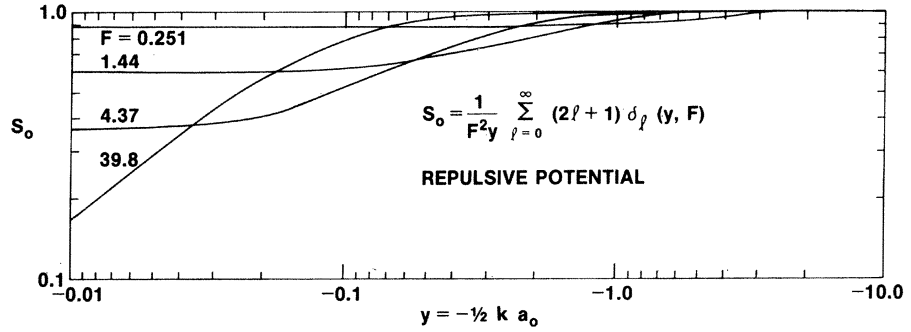

FIG. 1. $S_0(y,F)$ versus negative y (repulsive potential) for several constant values of F.

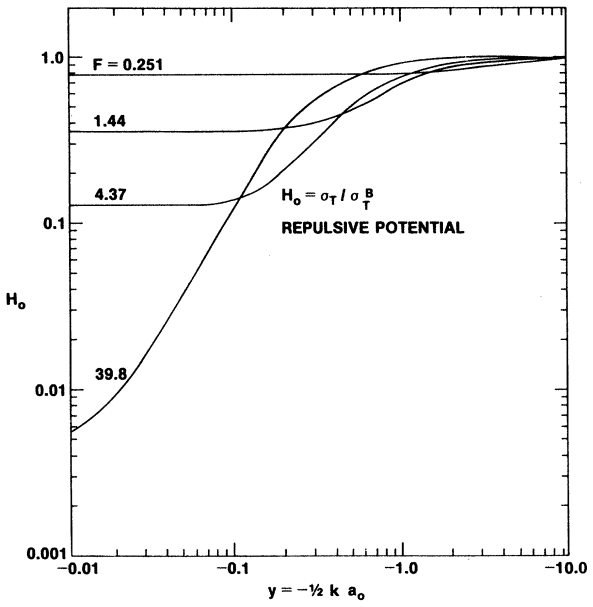

FIG. 2. $H_0(y,F)$ versus negative y (repulsive potential) for several constant values of F.

From Eq. (2.13), the potential is "weak" if $|y| \gg 1$. In this case the perturbed wave function will be very similar to the unperturbed result $[R_l \approx x j_l(x)]$, δ_l will be small, and Eq. (3.1) reduces to Eq. (2.27). That is, the Born approximation is valid for a sufficiently "weak" potential. Since S_0 and H_0 are normalized to Born results, these quantities must be close to unity in this regime, as is found to be the case in Figs. 1–6. On the other hand, for a "strong" potential ($|y| \ll 1$) the $U(x)$ term significantly influences the solution and R_l is very dissimilar from R_l^0. Here the Born approximation is invalid and S_0 and H_0 usually differ a great deal from unity.

Another aspect of interest is the "range" of the potential, as characterized by the quantity $b^{1/2}/2$. If the range is very short (i.e., $b^{1/2}/2 \ll 1$) and $l > 0$, the $l(l+1)/x^2$ term in Eq. (2.4) washes out $U(x) = (1/xy)\exp(-2x/b^{1/2})$ over its short range, and the term $U(x)$ has little effect on the wave function even when $|y|$ is quite small. Because $l(l+1)/x^2$ vanishes for $l = 0$, δ_0 is the only phase shift which must be considered here. It can be shown that in the limit of a strong, short-range potential, the zero-order phase shift has the form[19] $\delta_0(y,F) \xrightarrow[|y|\ll 1]{} A(F)y$. From Eq. (2.28), one then obtains $S_0 = A(F)/F^2$. That is, S_0 is independent of y in the limit of small y, as is illustrated in Figs. 1 and 3 (in Fig. 5, the small-y limit has not been reached at $y = 0.01$). Similarly, from Eq. (2.25) one obtains $H_0 \xrightarrow[y\ll 0]{} [A(F)/F^2]^2 = S_0^2$, as is seen from a comparison of Figs. 2 and 4 with Figs. 1 and 3. It can be shown that as the range of the potential is increased, terms up to[20] $l \approx b^{1/2}/2$ must be included in the sums of Eqs. (2.26) and (2.28). In some cases, the higher-order phase shifts can be approximated by the Born phase shifts, δ_{lB}.

We also point out the resonance peak which occurs for attractive potentials at small y near $F = 1.7$ (see Fig. 4). This is a quantum-mechanical effect which involves the existence of a bound

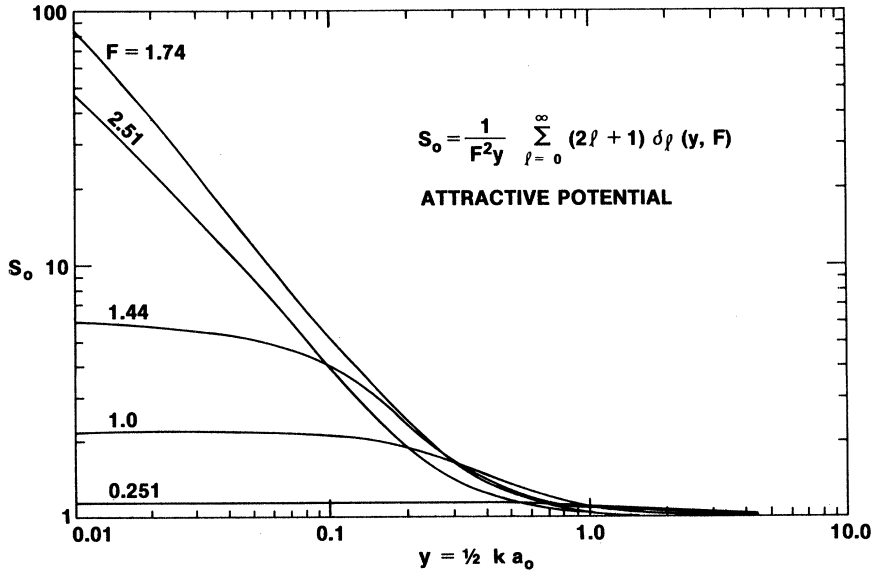

FIG. 3. $S_0(y,F)$ versus positive y (attractive potential) for several constant values of $F \leq 2.51$.

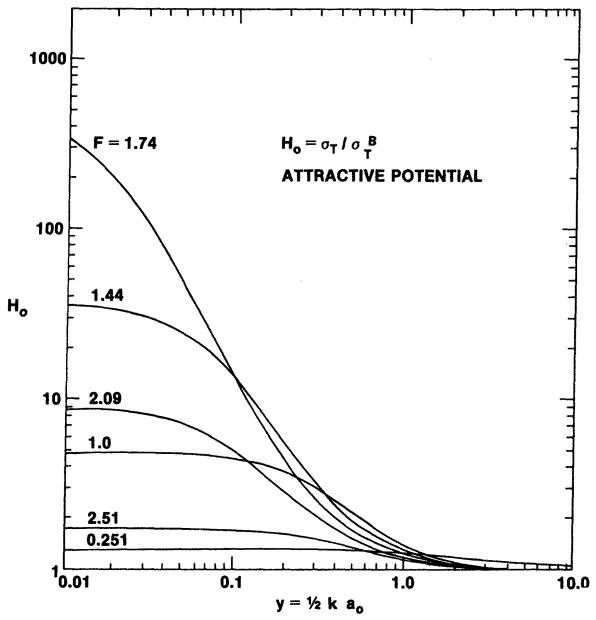

FIG. 4. $H_0(y,F)$ versus positive y (attractive potentia for several constant values of $F \leq 2.51$.

state with binding energy very close to zero.[21] If we approximate the screened Coulomb potential by a square well with depth $V_0 = Z_I e^2/\kappa_0 \lambda_s$ and width $a = \lambda_s$, the condition for resonance of the $l = 0$ partial wave in the low-energy limit is[21] $V_0 a^2 = (n + \frac{1}{2})^2 \pi^2 \hbar^2/2m^*$, which becomes $F = (n + \frac{1}{2})^2 \pi^2$. Thus the $n = 0$ resonance for a square well occurs at $F \approx 2.5$, which is close to the value observed in the figure. At $F = 1.74$, the phase-shift cross section for low y is over 100 times larger than the classical result, $\sigma_T = \pi \lambda_s^2$. Resonances for higher n and l are responsible for the oscillatory behavior at small y and large F.

Numerically derived phase shifts have been obtained in the past by several authors. The first was Blatt,[3] who obtained the total transport cross section as a function of two parameters ($k' = 31.5y^2$ and $R' = 0.178F$). While his approach was similar in some respects to that described above, the present calculation is much more comprehensive in several ways: (1) Blatt did not give a result equivalent to S_0, so that the Friedel sum rule could not be satisfied; (2) phase shifts were calculated only for $l \leq 5$, which caused relatively large error in some regions; (3) Blatt considered only the space $4.7 < F < 28$ and $0.018 < |y| < 5.6$, which excludes a number of experimentally interesting regions (the space covered in the present work is $0.1 \leq F < 400$ and $|y| \geq 0.01$) (4) Blatt gave only graphical results at sample values of his parameter R', so that it is extremely difficult to use his work in general transport calculations. The present results have been modeled to approximate analytic expressions with tabulated parameters, in addition to the graphical representations of Figs. 1–6.

Overall, Blatt's curves are in fair agreement with the present results, although they appear to be in error by as much as about 40% in some regions.

Krieger and Strauss[6] investigated the case of extremely degenerate electrons ($\eta_e \gg 1$) in a single band ($\nu_e = 1$) scattered by a singly ionized donor ($q_e Z_I = -1$), for which $y \to (\pi/2)/(\lambda_q F)^2$. Since there

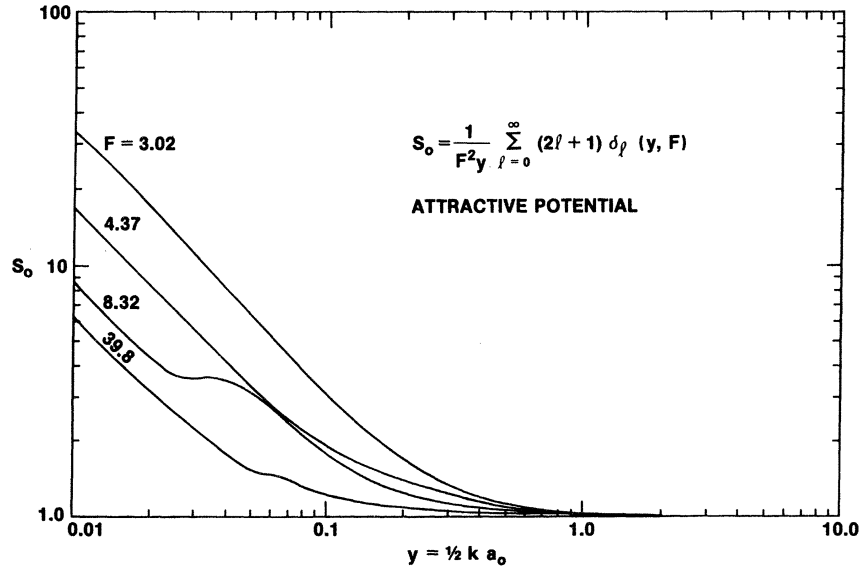

FIG. 5. $H_0(y,F)$ versus positive y (attractive potential) for several constant values of $F \geq 3.02$.

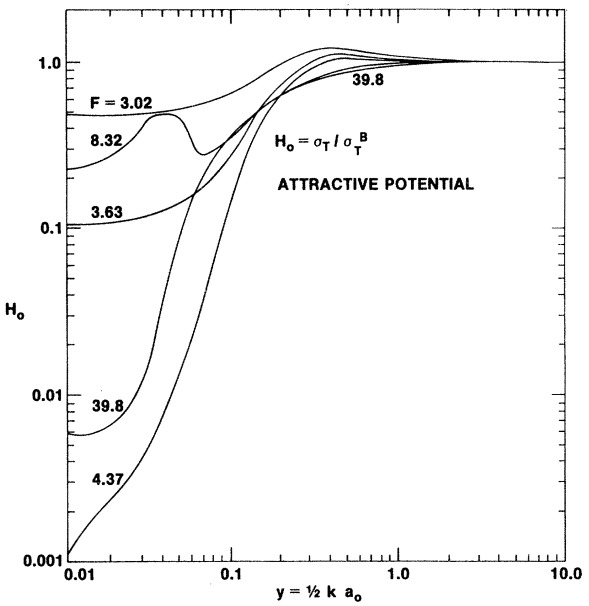

FIG. 6. $H_0(y,F)$ versus positive y (attractive potential) for several constant values of $F \geq 3.02$.

is then only one independent parameter, Krieger and Strauss were able to obtain a universal curve for the phase-shift resistivity divided by the Born resistivity as a function of $k_F a_0 (= 2y)$, where k_F is the Fermi wave vector. The curve obtained by Krieger and Strauss agrees to within 2% with the equivalent curve which can be generated using the present analytic models. Boardman and Henry[8] obtained numerical phase shifts in the nondegenerate regime. For the sample cases they considered, agreement with the present results is good.

IV. CALCULATION OF THE MOBILITY

We now demonstrate how electron and hole mobilities can be obtained from the numerically derived values of S_0 and H_0 which are given in the Appendix. It is emphasized that the mobilities calculated in this section are presented only for comparison with the Born approximation results. Since no mechanism besides ionized-impurity scattering is considered and compensation and carrier freeze-out are ignored, we do not attempt to compare with experimental data. A detailed transport model suitable for comparison with experiment is presented in a separate paper.[10]

Since we are considering only elastic scattering, the Boltzmann equation can be solved exactly in the relaxation-time approximation. For isotropic parabolic bands one obtains the following expression for the drift mobility[22]:

$$\mu = \frac{4e}{3\pi^{1/2} m^*_{\rm con} \mathfrak{F}_{1/2}(\eta)} \int z^{3/2} f_0 (1 - f_0) \tau(z) dz \,, \qquad (4.1)$$

where $m^*_{\rm con}$ is the "conductivity" effective mass and the relaxation time τ as a function of reduced energy z is given by

$$\tau^{-1}(z) = N_I v \sigma_T(y, F) \,. \qquad (4.2)$$

Here N_I is the density of ionized donors (n type) or acceptors (p type), $v = (2zk_BT/m^*)^{1/2}$ is the particle's velocity, and σ_T is the total momentum-transfer cross section for scattering by a screened Coulomb potential. In Sec. II we obtained $\sigma_T = \sigma_T^B H_0 (y, F)$, where the Born approximation result σ_T^B is given by Eq. (2.25) and H_0 is the correction obtained from the phase-shift calculation, which may be found from the approximate analytic expressions given in the Appendix. The parameters y and F are given by Eqs. (2.14) and (2.17). Before F can be evaluated, the adjustable screening parameter λ_q must be determined by satisfying the generalized Friedel sum rule, Eq. (2.29). The quantity $S_0(y(z), F(\lambda_q))$ can be found using expressions given in the Appendix.

Figure 7 shows the results of evaluating Eq. (4.1) numerically for a wide range of temperatures and doping levels in n-type germanium. (The appropriate material parameters are listed in Table I). The quantity plotted is the ratio between the phase-shift mobility and the Brooks-Herring result obtained using the Born approximation. At 300 K, the phase-shift correction is negligible for doping levels below 10^{17} cm^{-3}. This result can be obtained readily from the data summarized graphically in Figs. 5 and 6. In order to approximate λ_q so that F can be determined, we rewrite the sum rule Eq. (2.29). Assuming that the screening is by a single type of carrier (omit the sum over i), the equation can be evaluated in the Born approximation by setting $S_0 \to 1$ and $F^2 \to F_0^2$, where $F_0 \equiv 2\lambda_0/a_0$ and $F = F_0/\lambda_q$. Next, divide the left-

TABLE I. Material parameters.

	Ge[a]	Si[a]	GaAs[b]
κ_0	16.0	12.0	13.2
ν_e	4		1
m_e(con)	0.126		0.068
m_e(DS)	0.224		0.068
m_h		0.59	
m_l		0.16	

[a]M. Neuberger, *Handbook of Electronic Materials* (IFI/Plenum, New York, 1971), Vol. 5.

[b]M. Neuberger, *Handbook of Electronic Materials* (IFI/Plenum, New York, 1971), Vol. 2.

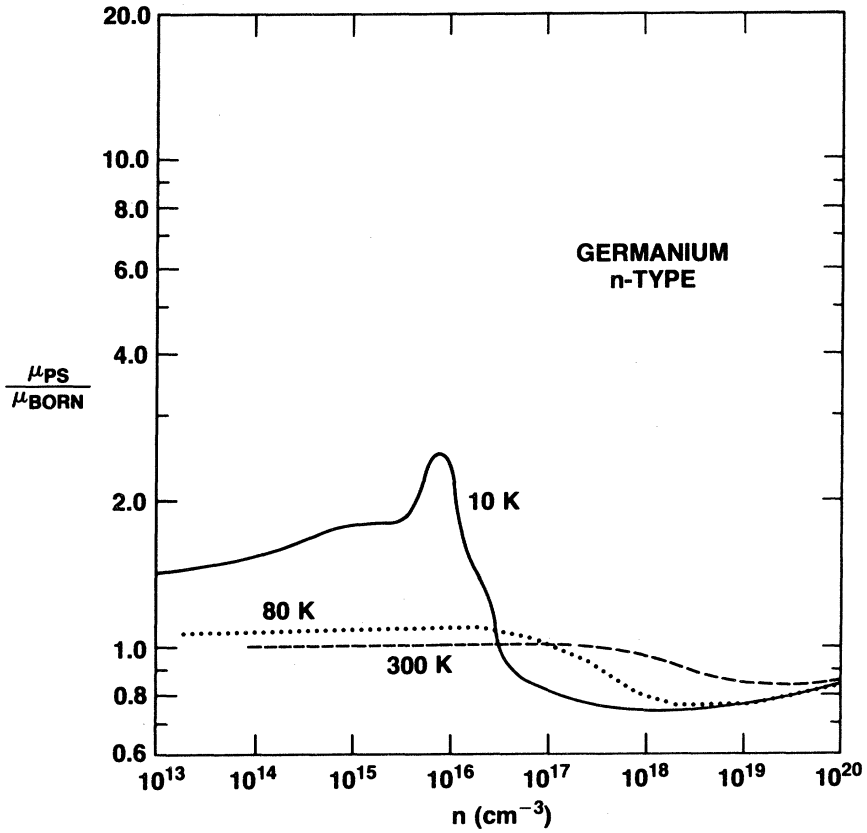

FIG. 7. Ratio of the phase-shift mobility to Brooks-Herring theory as a function of carrier density for three different temperatures in n-type germanium.

hand side and right-hand side of this new equation by the same sides of the general equation. One obtains

$$\lambda_q^2 = \langle S_0 \rangle \ , \tag{4.3}$$

where

$$\langle S_0 \rangle = \frac{\int_0^\infty dz\, f_0(1-f_0) y S_0(y(z), F(\lambda_q))}{\int_0^\infty dz\, f_0(1-f_0) y} \ . \tag{4.4}$$

As an approximation (which we recommend only for estimating purposes), one may use $\langle S_0 \rangle \approx S_0 (y(z_T), F_0)$, where z_T is an "average" reduced energy (for nondegenerate statistics $z_T \approx \frac{3}{2}$ and for degenerate statistics $z_T \approx \eta$). This approximation for $\langle S_0 \rangle$ should be reasonable as long as S_0 is not too rapidly varying and λ_q is not too large or too small. If we consider the specific case of $T \approx 300°$ K and $n = 10^{17}$ cm^{-3} in germanium, we can use the evaluations of y and F given by Eqs. (A1) and (A2) of the Appendix to obtain $y(z_T \approx \frac{3}{2}) \approx 0.9$ and $F_0 \approx 8.0$. From Fig. 5 we find that S_0 is close to unity, from which it follows that $\lambda_q \approx 1$. The ratio of the phase-shift mobility to the Brooks-Herring result can them be found by approximating the integral of Eq. (4.1) with the value of the integrand at $z = z_T$. Using Eq. (4.2) for $\tau(z_T)$, Eq. (2.25) for σ_T^B, and the relation $\sigma_T = H_0 \sigma_T^B$, one obtains

$$\frac{\mu_{PS}}{\mu_{Born}} \approx \frac{1}{H_0(y(z_T), F_0/\lambda_q)} \left(\frac{\ln(b_0+1) - b_0/(b_0+1)}{\ln(b+1) - b/(b+1)} \right), \tag{4.5}$$

where $b_0 \equiv 4y^2 F_0^2 = \lambda_q^2 b^2$ and both b and b_0 are evaluated at $z = z_T$. The ratio in brackets is due to the fact that the screening length is different for the phase-shift calculation than it is for Brooks-Herring. Figure 6 shows that $H_0(y = 0.9, F = 8.0)$ is also quite close to unity. Since $b_0 \to b$ when $\lambda_q \to 1$, we have determined that Brooks-Herring theory works well under these conditions. At lower carrier densities, S_0 and H_0 are approximated even better by unity.

However, if the carrier density is increased to $n = 10^{19}$ cm^{-3}, $y(z_T \approx 1.98) \approx 1.04$ while $F_0 \approx 0.92$. From Fig. 3, $S_0(y = 1.04, F = 0.92) \approx 1.16$, which implies $\lambda_q \approx 1.08$. The meaning of this result is as follows: That $S_0 > 1$ indicates that the phase shifts are larger than they had been in the Born

approximation. Thus in order to assure that the sum rule is still satisfied, we use a potential which is weaker than the Born potential. This is accomplished through increasing the effectiveness of the screening, that is, using λ_q greater than unity. From Fig. 4, $H_0(y = 1.04, F = 0.92/\lambda_q) \approx 1.42$, indicating that the scattering is 42% more effective that it would be in the Born approximation had both results employed the same screening length. However, since we are using the more strongly screened potential obtained above, the net mobility reduction as compared to Brooks-Herring theory is only about 24%, which can be obtained from Eq. (4.5). This result is shown in Fig. 7 for $T = 300$ K and $n = 10^{19}$ cm^{-3}.

Figure 7 also shows that while the behavior at 80 K is similar to that at 300 K, qualitative differences are evident at 10 K for low carrier densities. For example, at $n = 10^{15}$ cm^{-3}: $y \approx 0.17$ and $F_0 \approx 14.6$. This places one in the regions of Figs. 5 and 6 where not only is the potential weaker ($\lambda_q \approx 1.2$), but the cross section is also smaller than in the Born approximation for the same screening ($H_0 \approx 0.6$). Consequently, the phase-shift mobility is larger than Brooks-Herring by a factor of 1.8.

Figure 8 shows the results of a similar calculation for p-type silicon. Here one must take into account the presence of two different hole species, heavy holes and light holes with masses m_h and m_l listed in Table I. The composite mobility is $\mu_p = (n_h \mu_h + n_l \mu_l)/p$, where $p = n_h + n_l$ and $n_i/p = m_i^{3/2}/(m_h^{3/2} + m_l^{3/2})$, with $i = h$ or l. If we ignore interband scattering events, the mobilities μ_h and μ_l can each be found from Eq. (4.1). Since both types of carriers simultaneously screen the same impurity, a single λ_q characterizes all interactions. In Fig. 8, the high-temperature behavior is similar to that for n-type germanium. To understand the 10 K curve, consider the case of heavy holes at $p = 10^{16}$ cm^{-3}, where from Eqs. (A1) and (A2) of the Appendix $y_h \approx 0.08$ and $F_h \approx 14/\lambda_q \approx 8.8$, since $\lambda_q = 1.64$. This places one in the regime where H_0 shows large oscillations when either y or F is varied. Although the light-hole mobility is better behaved at this temperature since y_l is larger and F_l is smaller, the composite mobility is dominated by μ_h since $n_h \gg n_l$.

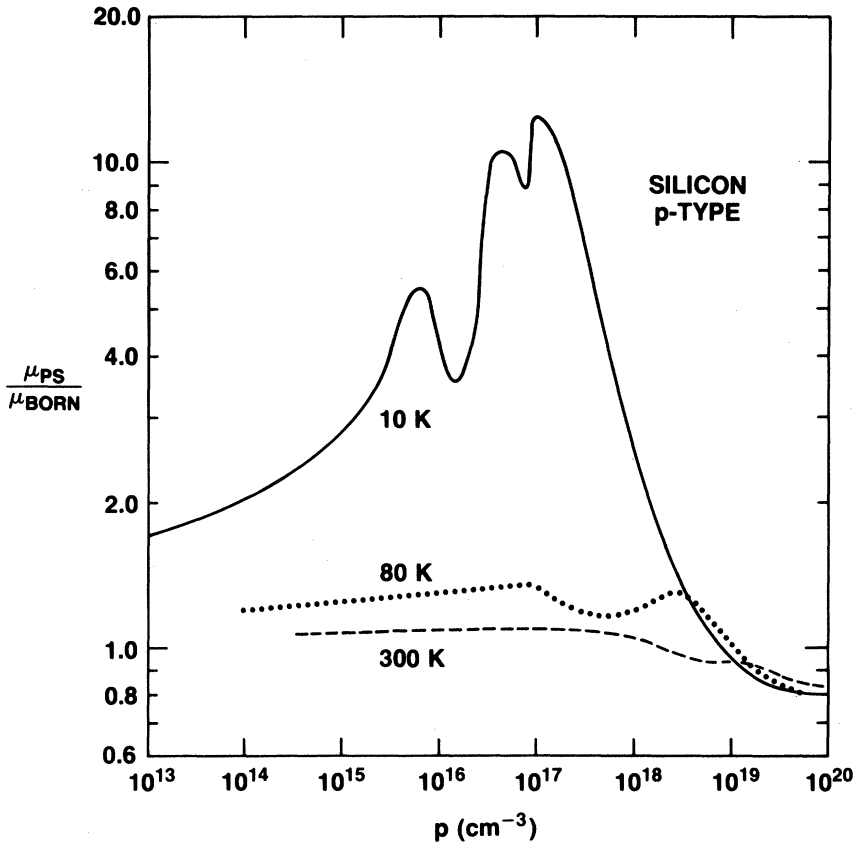

FIG. 8. Ratio of the phase-shift mobility to Brooks-Herring theory as a function of carrier density for three different temperatures in p-type silicon.

Considerations such as a randomness in the potential[3] or the anisotropy of the hole bands will smooth out any experimental peaks. Moreover, it is difficult to probe the conductivity at very low temperatures because of carrier freeze-out.

Figure 9 shows the results of the calculation for n-type GaAs. Since y is larger for the smaller electron mass of GaAs ($m_e \approx 0.068 m_0$) and $y \propto T^{1/2}$ for nondegenerate statistics, one must decrease the temperature to about 3 K before the oscillatory regime is reached. We emphasize again that Figs. 7–9 are in no way intended to be compared directly with experiment. A detailed mobility calculation must include a number of additional mechanisms, such as neutral impurity scattering, phonon scattering, electron-electron or hole-hole scattering, compensation, carrier freeze-out, and screening by electrons bound to donors. For n-type silicon, GaAs, and ZnSe at low temperatures, comprehensive comparisons between the available experimental data and the results of such a calculation are presented elsewhere.[10]

V. VALIDITY OF THE BORN APPROXIMATION

Over the years, a serious misconception has persisted concerning the criterion for validity of the Born approximation. In this section, we seek to clarify the misunderstanding.

In general, the Born approximation is valid if the electron wave function in the presence of the scattering potential is "similar" in form to the unperturbed wave function. It can be shown that for a spherically symmetric potential, this criterion is satisfied when[23]

$$u \equiv \frac{m^*}{\hbar^2 k}\left|\int_0^\infty V(r)(e^{2ikr}-1)dr\right| \ll 1 . \tag{5.1}$$

With $V(r) = (Z_I e^2/\kappa_0 r)\exp(-r/\lambda_s)$, the integral can be performed to yield[24]

$$u = \frac{1}{ka_0}\{[\ln(b+1)^{1/2}]^2 + (\tan^{-1}b^{1/2})^2\}^{1/2}$$

$$\xrightarrow[b\gg 1]{} \frac{\ln b}{2ka_0} = \frac{\ln b}{4|y|}$$

$$\xrightarrow[b\ll 1]{} \frac{b^{1/2}}{ka_0} = \frac{b^{1/2}}{2|y|} = F . \tag{5.2}$$

Since $\frac{1}{4}\ln b$ is on the order of unity for large b, we obtain in that limit the criterion[24]

$$|y| \gg 1 \quad (b \gg 1) . \tag{5.3}$$

Similarly in the small-b limit the Born approxima-

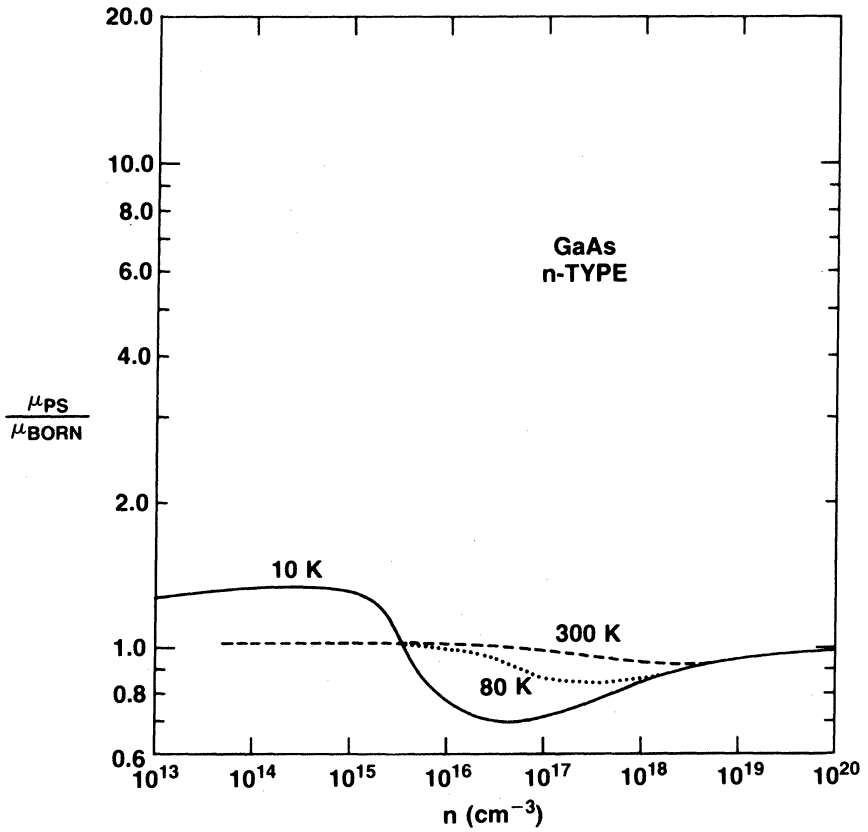

FIG. 9. Ratio of the phase-shift mobility to Brooks-Herring theory as a function of carrier density for three different temperatures in n-type GaAs.

tion is valid when $|y| \gg \frac{1}{2}b^{1/2}$, or

$$F \ll 1 \ (b \ll 1). \tag{5.4}$$

Combining the two results, we find the Born approximation is always valid when $|y|$ (or $\frac{1}{2}ka_0$) $\gg 1$, since in the small-b limit, $|y| \gg 1$ and $1 \gg \frac{1}{2}b^{1/2}$ imply inequality (5.4). Furthermore, while $|y| \gg 1$ is a sufficient condition for all b, at small b the Born approximation may also be valid for $|y| < 1$ as long as $F \ll 1$. These conclusions are illustrated in Figs. 1–6. The quantities $S_0(y, F)$ and $H_0(y, F)$ are always near unity when $|y| \gg 1$. They are also near unity whenever $F \ll 1$, even at small $|y|$. Recall from Sec. III that the quantity $|y|^{-1}$ characterizes the "strength" of the interaction potential $U(x)$. The present result confirms the assertion made in that section that the Born approximation should be valid for a "weak" potential

The criterion

$$b \gg 1 \tag{5.5}$$

has frequently been used to justify the use of Brooks-Herring theory. While this criterion is appropriate for degenerate semiconductors,[25] it has been applied by a number of authors[26–29] to cases governed by nondegenerate statistics. In these instances, reference is often made to an assertion by Blatt[30] that the validity of the Born approximation implies $b \gg 1$ (Sclar[24] had earlier made a similar observation). While this statement usually holds, the converse is by no means generally true. A criterion which is valid for arbitrary degeneracy can be obtained if we rewrite inequality (5.3) as $b^{1/2}/2F \gg 1$, or

$$b \gg 4F^2. \tag{5.6}$$

Since F is usually large for nondegenerate carrier populations, inequality (5.5) is clearly incorrect as a general criterion. As an example, we note that for n-type germanium at 10 K with $N_D = 10^{13}$ cm^{-3}, $N_A = 0$, and $z = \hbar^2k^2/2m^*k_BT \approx \frac{3}{2}$, one obtains $b = 1300$ and $F = 142$. While inequality (5.5) is easily satisfied, inequality (5.6) does not hold, since $4F^2 \approx 80\,000$. It can be seen from Fig. 7 that the use of Brooks-Herring theory in this example causes error of more than 40%.

VI. CONCLUSIONS

It has been nearly twenty five years since the partial-wave phase-shift formalism was first applied to the scattering of free electrons in a semiconductor by a screened Coulomb potential. The approach has clear advantages over the Born approximation in that one can obtain highly accurate scattering cross sections for potentials of any strength and range. However, beyond certain specific regimes it has not been possible to apply previously published results to the calculation of electron and hole mobilities for arbitrary experimental conditions.

In the phase-shift formalism, the scattering problem can be considered generally in terms of two universal parameters, which we call y and F. For an extensive space in these parameters we have obtained the two final results required to

TABLE II. $a_i(F)$ and $b_i(F)$ to be used in Eqs. (A4) and (A5) for $y \leq -0.01$. The maximum modeling error is given by Eq. (A6), where $\epsilon_S \leq 0.011$ and $\epsilon_H \leq 0.019$ in this range.

$\log_{10}(F)$	F	a_0	a_1	a_2	b_0	b_1	b_2
−1.00	0.100	−20.72	0.9023	−0.8724	−10.23	−0.077 23	−0.1382
−0.80	0.158	−13.35	0.6619	−1.362	−6.611	−0.039 06	−0.2197
−0.60	0.251	−8.657	0.5328	−2.184	−4.285	−0.053 86	−0.3311
−0.40	0.398	−5.676	0.3214	−3.389	−2.816	−0.054 00	−0.5025
−0.20	0.631	−3.793	0.1025	−5.247	−1.888	−0.042 16	−0.7601
0.00	1.00	−2.598	−0.1680	−8.097	−1.297	−0.023 26	−1.137
0.20	1.58	−1.831	−0.5610	−12.44	−0.9183	−0.012 30	−1.663
0.40	2.51	−1.313	−1.830	−16.55	−0.6713	−0.021 87	−2.373
0.60	3.98	−0.9973	−2.203	−28.54	−0.5060	−0.083 35	−3.276
0.80	6.31	−0.7673	−3.790	−42.26	−0.3910	−0.240 9	−4.338
1.00	10.0	−0.5967	−6.403	−60.30	−0.3077	−0.540 4	−5.472
1.20	15.8	−0.4847	−9.585	−87.45	−0.2453	−1.030	−6.495
1.40	25.1	−0.4131	−13.33	−130.1	−0.1987	−1.699	−7.377
1.60	39.8	−0.3745	−17.40	−201.3	−0.1657	−2.506	−8.193
1.80	63.1	−0.3616	−21.64	−321.8	−0.1443	−3.393	−9.190
2.00	100.0	−0.3699	−25.87	−526.7	−0.1308	−4.397	−10.24
2.20	158.0	−0.3987	−29.64	−878.3	−0.1229	−5.528	−11.61
2.40	251.0	−0.4552	−31.53	−1498.0	−0.1170	−6.957	−12.06
2.60	398.0	−0.5685	−27.05	−2663.0	−0.1131	−8.665	−12.18

TABLE III. $a_i(F)$ and $b_i(F)$ to be used in Eqs. (A4) and (A5) for $y \leq 0.01$ ($\epsilon_S \leq 0.024, \epsilon_H \leq 0.016$).

$\log_{10}(F)$	F	a_0	a_1	a_2	b_0	b_1	b_2
−1.00	0.100	19.10	0.893 0	0.7364	9.654	0.047 54	0.1507
−0.80	0.158	11.85	0.529 0	1.204	5.948	0.091 24	0.2335
−0.60	0.251	7.280	0.118 6	2.051	3.621	0.136 8	0.3657
−0.40	0.398	4.349	−0.055 98	3.307	2.152	0.187 4	0.5889
−0.20	0.631	2.478	−0.160 1	5.319	1.219	0.269 1	0.9787
−0.16	0.692	2.194	−0.173 2	5.843	1.077	0.296 1	1.087
−0.12	0.759	1.934	−0.198 4	6.472	0.9462	0.327 0	1.211
−0.08	0.832	1.694	−0.202 3	7.130	0.8261	0.366 9	1.350
−0.04	0.912	1.473	−0.186 6	7.844	0.7153	0.415 7	1.510
0.00	1.00	1.264	−0.120 4	8.594	0.6151	0.463 6	1.704
0.04	1.10	1.073	−0.057 51	9.451	0.5198	0.544 9	1.911
0.08	1.20	0.8934	0.058 52	10.39	0.4301	0.659 3	2.141
0.12	1.32	0.7206	0.268 4	11.33	0.3443	0.833 2	2.378
0.16	1.45	0.5483	0.692 8	12.07	0.2594	1.128	2.562
0.20	1.58	0.3600	1.748	11.51	0.1691	1.765	2.359
0.24	1.74	0.1978	3.522	8.066	0.1479	2.202	2.369
0.28	1.91	0.2017	3.168	10.46	0.2614	1.785	3.530
0.32	2.09	0.2103	3.203	12.05	0.4180	1.893	3.918
0.36	2.29	0.2176	3.482	13.42	0.7172	2.220	3.956
0.40	2.51	0.2241	3.928	14.91	1.719	0.936 0	4.910

perform a calculation of the transport properties. One, called $S_0(y, F)$, is needed to assure that the generalized Friedel sum rule is satisfied. The other, $H_0(y, F)$, is the total momentum-transfer scattering cross section in units of the Born approximation result. Using the approximate analytic expressions for S_0 and H_0 given in the Appendix, one can calculate ionized-impurity mobilities for almost any desired experimental conditions. As examples, results for n-type germanium, p-type silicon, and n-type GaAs at a broad range of carrier densities and temperatures have been compared with mobilities obtained from Brooks-Herring theory. It is found that in general, Brooks-Herring tends to underestimate the phase-shift mobility in regions governed by nondegenerate statistics and to overestimate it when degenerate statistics apply. It is also observed that Brooks-Herring tends to be less accurate for a carrier species with a large effective mass. The two mobilities agree when the Born approximation is valid, which occurs when either $|y| \gg 1$ or $F \ll 1$. In many regions of experimental interest, neither of these conditions is satisfied and the use of Brooks-Herring theory can cause serious error. Although the present mobility results are not suitable for direct comparison with experiment since scattering mechanisms other than ionized impurities have not been included, a detailed transport theory is presented in a separate paper.[10]

APPENDIX: MODELING OF $S_0(y,F)$ AND $H_0(y,F)$

The results of the phase-shift calculation can be summarized in terms of two quantities, $S_0(y,F)$ and $H_0(y,F)$, which are defined by Eqs. (2.28) and (2.26), respectively. The two universal parameters y and F are given by

TABLE IV. $c_i(y)$ and $d_i(y)$ to be used in Eqs. (A7) and (A8) for $2.51 \leq F \leq 398$ ($\epsilon_S, \epsilon_H \leq 0.011$).

$\log_{10}(y)$	y	c_0	c_1	c_2	d_0	d_1	d_2
0.6	3.98	0.003 359	−0.019 71	0.019 58	0.010 90	−0.051 77	0.089 68
0.4	2.51	0.002 201	−0.016 36	0.032 18	0.002 569	−0.050 33	0.151 7
0.2	1.58	0.000 136	−0.006 783	0.053 07	0.007 962	−0.156 3	0.398 1
0.0	1.00	−0.001 265	0.004 242	0.105 6	−0.017 98	−0.236 4	0.750 7
−0.2	0.631	−0.002 889	0.024 61	0.221 9	−0.056 48	−0.514 6	1.538
−0.4	0.398	−0.005 619	0.073 87	0.442 0	−0.101 8	−1.166	2.935

TABLE V. $c_i(y)$ and $d_i(y)$ to be used in Eqs. (A7) and (A8) for $2.51 \leq F \leq 4.79$, along with the maximum $\epsilon_{S,H}$ for each y.

$\log_{10}(y)$	y	c_0	c_1	c_2	d_0	d_1	d_2	ϵ_S	ϵ_H
−0.6	0.2512	0.7033	−2.674	3.610	2.993	−14.80	17.07	0.001	0.003
−0.8	0.1585	1.603	−6.529	8.474	6.995	−34.47	38.39	0.003	0.014
−1.0	0.1000	0.2591	−2.154	6.213	−2.634	−8.687	21.81	0.004	0.016
−1.2	0.0631	−1.659	5.260	0.6190	−31.25	84.38	−54.00	0.002	0.026
−1.4	0.0398	−2.465	9.360	−2.557	−52.62	154.5	−111.6	0.002	0.049
−1.6	0.0251	−2.653	11.49	−4.211	−47.01	133.3	−91.93	0.001	0.156
−1.8	0.0158	−2.569	12.74	−5.185	−42.70	117.4	−77.47	0.001	0.298
−2.0	0.0100	−2.348	13.54	−5.819	−40.35	109.0	−69.94	0.001	0.474

$$y(z) = -\frac{1}{2} k a_0 \frac{|Z_I|}{q_i Z_I} = -0.349 \frac{z^{1/2}}{q_i Z_i} \left(\frac{\kappa_0}{16}\right) \left(\frac{m^*_{DS}}{m_0}\right)^{-1/2} \left(\frac{T}{300}\right)^{1/2} \tag{A1}$$

$$F = 2\lambda_s/a_0 = 3570 \frac{|Z_I|}{\lambda_q} \left(\frac{\kappa_0}{16}\right)^{-1/2} \left(\frac{m^*_{DS}}{m_0}\right) \left(\frac{n}{10^{13}}\right)^{-1/2} \left(\frac{T}{300}\right)^{1/2} \left(\frac{\mathfrak{F}_{1/2}(\eta)}{\mathfrak{F}_{-1/2}(\eta)}\right)^{1/2}. \tag{A2}$$

For convenience, we also evaluate the related parameter b:

$$b(z) = 4k^2\lambda_s^2 = 4F^2y^2 = (6.21 \times 10^6) \frac{z}{\lambda_q^2} \left(\frac{\kappa_0}{16}\right) \left(\frac{m^*_{DS}}{m_0}\right) \left(\frac{n}{10^{13}}\right)^{-1} \left(\frac{T}{300}\right)^2 \left(\frac{\mathfrak{F}_{1/2}(\eta)}{\mathfrak{F}_{-1/2}(\eta)}\right). \tag{A3}$$

The effective mass has been written m^*_{DS} to indicate that in cases such as n-type germanium and silicon, the "density-of-states" effective mass should be employed rather than the "conductivity" effective mass m^*_{con}.[31] [Were m^*_{con} to be employed in Eqs. (A1) and (A2), the generalized Friedel sum rule Eq. (2.29) would not be satisfied in the Born approximation.]

Values of S_0 and H_0 for $|y| \geq 0.01$ and $0.1 \leq F \leq 398$, have been fit to approximate analytic expressions by subdividing this area of y-F space. For $y \leq -0.01$ (and certain positive y specified below), results have been fit to the following forms:

$$S_0(y,F) = \exp\{[a_0(F) + a_1(F)|y| + a_2(F)y^2]^{-1}\} \tag{A4}$$

and

$$H_0(y,F) = \exp\{[b_0(F) + b_1(F)|y| + b_2(F)y_2]^{-1}\}, \tag{A5}$$

where the six parameters $a_i(F)$ and $b_i(F)$ are given in Table II for values of F between 0.1 and 398. These forms are well suited to the functions since they asymptotically yield unity for $|y| \gg 1$ and are independent of y at $|y| \ll 1$.

We can define the relative error E which is introduced by the modeling as follows: $E = |A - A_m|/A$, where A is the value for S_0 or H_0 which is calculated directly from the phase shifts, and A_m is the approximate value given by the model. The actual error characterization will be given in terms of the error parameter $\epsilon_{S,H}$ which is related to E by

$$\epsilon_{S,H} = \frac{E}{1 + 3|\ln A|}. \tag{A6}$$

TABLE VI. $c_i(y)$ and $d_i(y)$ to be used in Eqs. (A7) and (A8) for $4.79 \leq F \leq 10$, along with the maximum $\epsilon_{S,H}$ for each y.

$\log_{10}(y)$	y	c_0	c_1	c_2	d_0	d_1	d_2	ϵ_S	ϵ_H
−0.6	0.2512	−0.07895	0.6326	0.1180	−0.6267	0.7699	0.3403	0.001	0.001
−0.8	0.1585	−0.5574	3.740	−3.644	−4.434	20.38	−26.73	0.002	0.006
−1.0	0.1000	−0.8910	7.138	−8.711	−19.33	100.7	−137.9	0.013	0.033
−1.2	0.0631	4.036	−16.26	20.25	−47.89	257.3	−355.9	0.032	0.077
−1.4	0.0398	11.07	−51.20	65.22	−90.55	481.3	−644.7	0.029	0.175
−1.6	0.0251	13.86	−64.40	83.05	−116.3	605.5	−789.3	0.051	0.124
−1.8	0.0158	14.55	−65.34	83.91	−134.9	699.1	−904.0	0.057	0.234
−2.0	0.0100	14.89	−64.27	82.03	−140.9	728.8	−939.6	0.048	0.405

TABLE VII. $c_i(y)$ and $d_i(y)$ to be used in Eqs. (A7) and (A8) for $10 \leq F \leq 398$, along with the maximum ϵ_S and ϵ_H.

$\log_{10}(y)$	y	c_0	c_1	c_2	d_0	d_1	d_2	ϵ_S	ϵ_H
−0.6	0.2512	−0.010 71	0.1902	0.8442	−0.173 1	−2.133	5.031	0.001	0.005
−0.8	0.1585	−0.023 17	0.5173	1.227	−0.264 1	−3.382	6.953	0.001	0.007
−1.0	0.1000	−0.042 87	1.194	1.423	−0.430 7	−4.186	4.729	0.002	0.009
−1.2	0.0631	−0.056 57	2.196	1.705	−0.464 2	−8.649	8.836	0.012	0.018
−1.4	0.0398	−0.051 70	3.680	0.9815	−0.013 82	−25.90	54.13	0.037	0.095
−1.6	0.0251	−0.046 13	6.338	−2.853	−0.318 8	−37.73	96.94	0.040	0.277
−1.8	0.0158	0.029 75	9.271	−8.679	−2.691	−19.37	63.81	0.052	0.364
−2.0	0.0100	0.233 8	11.47	−13.24	−5.371	6.117	10.65	0.051	0.371

The purpose of the weighting factor $1+3|\ln A|$ is to require the model to be much more accurate in regions where the Born approximation is nearly valid than in regions where S_0 and H_0 are very different from unity. We illustrate by noting that from Table II $\epsilon_S(y \leq -0.01) \leq 0.011$. From Eq. (A6), this means that when $A = S_0 \approx 1.0$, the maximum relative error E is 0.011, or 1.1%. However, if $S_0 = 10$ or 0.1, the maximum error can be as large as $1+3\ln 10 \approx 8.7\%$. Of course, the value $\epsilon_S = 0.011$ given in Table II is a maximum for the entire space $y \leq -0.01$ and the actual error is much smaller than this in most regions. The use of a numerical technique such as four-point Gaussian interpolation[32] to evaluate S_0 at values between those given in Table II should contribute little additional error. For $H_0(y<0,F)$, the maximum error is only slightly higher, as characterized by $\epsilon_H \leq 0.019$.

For the range $y \geq 0.01$ and $0.1 \leq F \leq 2.51$, S_0 and H_0 have also been fit to expressions (A4) and (A5), where the parameters $a_i(F)$ and $b_i(F)$ are given in Table III for F values in this range. Since S_0 and H_0 are relatively well behaved in this region, the modeling error is modest ($\epsilon_S \leq 0.024$, $\epsilon_H \leq 0.016$).

For $y \geq 0.01$ and $2.51 \leq F \leq 398$, S_0 and H_0 have been fit to the following forms:

$$S_0(y,F) = \exp[c_0(y) + c_1(y)/F^{1/2} + c_2(y)/F] \quad \text{(A7)}$$

and

$$H_0(y,F) = \exp[d_0(y) + d_1(y)/F^{1/2} + d_2(y)/F]. \quad \text{(A8)}$$

Because of the less well-behaved nature of the functions S_0 and H_0 at large F, it is necessary to further break the (y,F) space into several regions. For $y \geq 0.398$, a single set of values for $c_i(y)$ and $d_i(y)$ can be used for the entire range $2.51 \leq F < 400$. These are given in Table IV for y values between 0.398 and 3.98 (when $y > 3.98$, S_0, and H_0 approach unity, as seen in Figs. 5 and 6). In the range covered by Table IV $\epsilon_S, \epsilon_H \leq 0.011$. As y decreases below 0.398, one enters the oscillatory regime of Fig. 6. Here Eqs. (A7) and (A8) must be used in three F segments for each y. The parameters $c_i(y)$ and $d_i(y)$, along with the maximum values of $\epsilon_{S,H}(y)$ for the three segments are given in Tables V–VII. Because of the strong oscillatory behavior at small y and large F, accurate modeling is very difficult in this region (a prohibitively large amount of tabular material would be required). Fortunately, this regime is not easily reached experimentally.

[1] H. Brooks, Phys. Rev. 83, 879 (1951).
[2] C. Herring (unpublished).
[3] F. J. Blatt, J. Phys. Chem. Solids 1, 262 (1957).
[4] P. Csavinszky, Phys. Rev. 126, 1436 (1962).
[5] J. Friedel, Adv. Phys. 3, 446 (1954).
[6] J. B. Krieger and S. Strauss, Phys. Rev. 169, 674 (1968).
[7] Actually, a second parameter is introduced if one varies the conduction-band valley degeneracy or the charge of the impurity. Krieger and Strauss assumed both to be unity.
[8] A. D. Boardman and D. W. Henry, Phys. Status Solidi B 60, 633 (1973).
[9] F. Stern, Phys. Rev. 158, 697 (1967).
[10] J. R. Meyer and F. J. Bartoli (unpublished).
[11] L. I. Schiff, *Quantum Mechanics* (McGraw-Hill, New York, 1968), 3rd ed., p. 119.
[12] K. Huang, Proc. Phys. Soc. London 60, 161 (1948).
[13] R. B. Dingle, Philos. Mag. 46, 831 (1955). We call this the Born approximation result because the generalized Friedel sum rule Eq. (2.22) is not satisfied for Born approximation phase shifts unless the screening length has this value.
[14] The carrier density is related to $\mathfrak{F}_{1/2}$ as follows: $\mathfrak{F}_{1/2}(\eta) = (4n/\nu)(\pi\hbar^2/2m_{DS})^{3/2}$.
[15] J. M. Ziman, *Principles of the Theory of Solids* (Cam-

bridge University Press, Cambridge, 1965), p. 135.
[16]M. Abramowitz and I. A. Stegun, *Handbook of Mathematical Functions* (National Bureau of Standards, Washington, D. C., 1964), p. 437.
[17]L.I. Schiff, *Quantum Mechanics* (McGraw-Hill, New York, 1968), 3rd ed., p. 330.
[18]It can be shown that in the Born approximation, the sum rule is satisfied when the screening parameter λ_q is set to unity. Note also that in the extreme degenerate limit $S^B \to -(q_i Z_I/\nu)\pi/2$.
[19]The function $A(F)$ can apparently not be determined analytically.
[20]A. S. Davydov, *Quantum Mechanics* (Pergamon, New York, 1965), p. 389.
[21]See Ref. 17, p. 128.
[22]K. Seeger, *Semiconductor Physics* (Springer, New York, 1973), p. 55.
[23]See Ref. 20, p. 378.
[24]N. Sclar, Phys. Rev. 104, 1548 (1956).
[25]Under conditions of extreme degeneracy, one may use the relation $ka_0 \xrightarrow[\eta \gg 1]{} b\nu/|Z_I|\pi$ with inequality (5.3) to obtain the criterion $b \gg 2\pi|Z_I|/\nu$, which is approximately equivalent to inequality (5.5).
[26]D. L. Long and J. Myers, Phys. Rev. 115, 1107 (1959).
[27]A. C. Beer, *Galvanomagnetic Effects in Semiconductors* (Academic, New York, 1963), p. 112.
[28]D. L. Rode and S. Knight, Phys. Rev. B 3, 2534 (1971); D. L. Rode, in *Semiconductors and Semimetals*, Vol. 10, edited by R. K. Willardson and A. C. Beer (Academic, New York, 1975), p. 1.
[29]J. L. Blankenship, Phys. Rev. B 7, 3725 (1973).
[30]F. J, Blatt, Phys. Rev. 105, 1203 (1957); Solid State Phys. 4, 199 (1957).
[31]The two masses are defined

$$m_{DS}^* = m_1^{2/3} m_3^{1/3}, \quad m_{con}^* = \left(\frac{2}{3m_1} + \frac{1}{3m_3}\right)^{-1},$$

where m_1 and m_3 are the transverse and longitudinal masses, respectively.
[32]M. Abramowitz and I. A. Stegun, *Handbook of Mathematical Functions* (National Bureau of Standards, Washington, D. C., 1964), p. 437.